ISSN 1063-7710, Acoustical Physics, 2013, Vol. 59, No. 5, pp. 528–532. © Pleiades Publishing, Ltd., 2013.

PHYSICAL ACOUSTICS

Study on Sensitivities of Love-Wave Immunosensors Based on SiO_2/36°YX-$LiTaO_3$ and ZnO/36°YX-$LiTaO_3$ Structures[1]

Ming-tai Song, Shu-yi Zhang, Li Fan, Feng-mei Zhou, Yan Wang, and Xiu-ji Shui

Lab of Modern Acoustics, Institute of Acoustics, Nanjing University, Nanjing 210093, PR China

e-mail: zhangsy@nju.edu.cn

Received November 19, 2012

Abstract—Love-wave immunosensors based on SiO_2/36°YX-$LiTaO_3$ or ZnO/36°YX-$LiTaO_3$ structures coated by special sensitive films have been fabricated and studied experimentally. A theoretical model using the partial wave theory of elastic waves propagating in three-layer structures covered by liquid loads is built up to calculate the sensitivities. To determine the elastic constants of the guiding layers, the phase velocities of the corresponding Love-wave devices are measured by a network analyzer, and the theoretical fitting of the experimental data are carried out. Then the relationships between the sensitivities of the Love-wave immunosensors and normalized thicknesses of the guiding layers are obtained, and there are optimized thicknesses of the guiding layers for getting maximum sensitivities. The experimental measurements and numerical calculations of the sensitivities of the Love-wave immunosensors show that both results are essentially consistent with each other.

Keywords: Love-wave device, guiding layer, elastic constant, immunosensor, sensitivity

DOI: 10.1134/S1063771013050217

1. INTRODUCTION

Surface acoustic wave (SAW) devices have been used widely as sensors in gaseous and liquid environments [1–4]. For sensing devices in liquid environment, shear horizontal (SH) polarized waves are used instead of Rayleigh waves, because SH waves do not have elastic coupling with liquids and so make no radiation losses [5, 6]. The SH mode can be converted into Love mode by covering a thin layer on the top of the substrate acting as a waveguide, but the shear velocity of the guiding layer must be smaller than that of the substrate. Resulting from the waveguide effect, the Love waves can be very sensitive to surface perturbations, and then high sensitivities can be achieved [7, 8].

As guiding layer materials, SiO_2 and ZnO overlays have been always used because of their excellent properties: low shear velocity, low acoustic absorption, high chemical stability, etc. [9, 10]. The experimental results show that the Love-wave immunosensors based on SiO_2/36°YX-$LiTaO_3$ and ZnO/36°YX-$LiTaO_3$ structures have very high sensitivities. But the sensitivities are strongly dependent on the thicknesses of the guiding layers, and there are optimum thicknesses for getting maximum sensitivities [11, 12].

In this work, the Love-wave immunosensors based on SiO_2/36°YX-$LiTaO_3$ and ZnO/36°YX-$LiTaO_3$ structures coated by special sensitive films have been fabricated and their sensitivities have been measured experimentally. Meanwhile, a theoretical model using the partial wave theory of elastic waves propagating in three-layer structures covered by liquid loads is built up to calculate the sensitivities. To numerically evaluate the sensitivities of the immunosensors, the phase velocities of the corresponding Love-wave devices are measured and the theoretical fitting of the experimental data are carried out to evaluate the elastic constants of the guide layers. Then the relationships between the sensitivities of the Love-wave immunosensors and normalized thicknesses of the guiding layers are obtained in theory, which are in agreement with that of the experiments.

[1] The article is published in the original.

2. EXPERIMENT

The Love-wave devices have been fabricated on 36°YX-$LiTaO_3$ substrates, on which the transmitting and receiving interdigital transducers (IDTs) with Au electrodes consist of 90 finger pairs with the period 32 μm and aperture 2.5 mm, and the distance of the center-to-center of both IDTs is 245 λ_0 (λ_0 is the period). The SiO_2 or ZnO guiding layers of different thicknesses are then deposited on the substrates by RF magnetron sputtering technique [12]. The deposition conditions are listed in Table 1.

For the Love wave immunosensors either base on the SiO_2/36°YX-$LiTaO_3$ or ZnO/36°YX-$LiTaO_3$ structures, the surfaces of the devices are coated by special thin sensing films for binding the detected analysts, such as the sensing film is antibody and the detected analyst is antigen or vice versa.

Table 1. Deposition condition of guiding layer

Layer	Target	Sputtering gas	Substrate temperature	Deposition pressure	RF power
SiO_2	Si wafer	Ar(50%) + O_2(50%)	Room temperature	1 Pa	80 W
ZnO	ZnO powder	Ar(50%) + O_2(50%)	400°C	0.5 Pa	70 W

The operating frequencies of the Love-wave devices based on SiO_2/36°YX-$LiTaO_3$ and ZnO/36°YX-$LiTaO_3$ structures can be measured by two methods as shown in Fig.1. In one method, a network analyzer is used to measure the frequency, phase and insertion loss quickly, and the other is a oscillating closed-loop consisted of a broadband amplifier and a frequency counter, which is used to measure the frequencies more accurately, but may be easily influenced by the environment [12, 13]. Generally, both methods are used to check the results with each other.

2.1. Experimental Evaluation of Elastic Constant of Guiding Layer

To theoretical evaluate the sensitivity of the Love wave immunosensors, the elastic constants of the guiding layers must be determined since the elastic constants of thin layers are always quite different from their corresponding bulk materials. Generally, the elastic constants can be determined by the velocities of waves in the Love wave devices.

When the thickness of the deposited SiO_2 or ZnO guiding layer is changed, the frequency variations of the Love-wave devices are measured. Based on the IDT period and the frequency variations, the phase velocity variations of waves in the Love-wave devices with the different normalized thicknesses of the guiding layer can be obtained experimentally as shown in Fig. 2. According to the theoretical relations between the phase velocities and the related parameters of the guiding layer and substrate, the elastic constants of the guiding layer can be evaluated.

2.2 Experimental Measurement of Sensitivity of Love-wave Immunosensor

The gravimetric sensitivity of surface acoustic wave sensors is defined by [9, 14]:

$$S = \lim_{\Delta m \to 0} \frac{1}{\Delta m} \frac{\Delta f}{f_0} = \lim_{\Delta m \to 0} \frac{1}{\Delta m} \frac{\Delta v}{v_0},$$

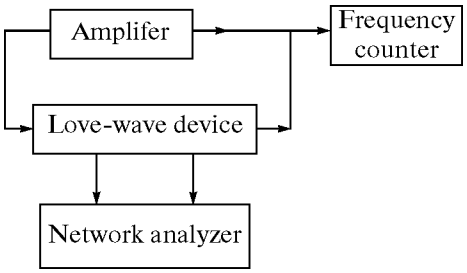

Fig. 1. Schematic diagram of experimental system.

where Δm is a small perturbation of the mass per surface area, $\Delta f = f_1 - f_0$, $\Delta v = v_1 - v_0$, and f_s and v_s (s = 0, 1 represent loaded and unloaded conditions) are the frequency and phase velocity of the surface acoustic wave in devices respectively.

For measuring the sensitivity of the Love wave immunosensors, human immunoglobulin G (H IgG) is chosen as the investigated antigen, and protein A coupled with human antibody immunoglobin G (anti-H IgG) is chosen to work as sensing film to bind H IgG. For immobilizing the protein A and then the H anti-IgG molecular layer, Au(50 nm)/Cr(20 nm) films are first deposited on the surface area of the Love-wave device between both IDTs. A teflon cell with a volume about 150 μL is adhered on the surface area of the device for holding the related solutions involving the protein A and anti-H IgG solutions in the sensing films preparation process and then the H IgG solution in the sensing experiments. As an example, the sensing experiment can be described briefly as follows [12].

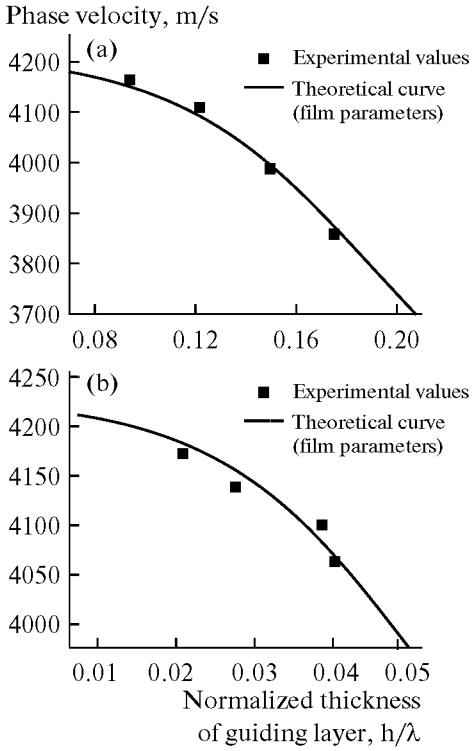

Fig. 2. Experimental phase velocity of Love-wave device versus normalized thickness of guiding layer: (a) SiO_2; (b) ZnO.

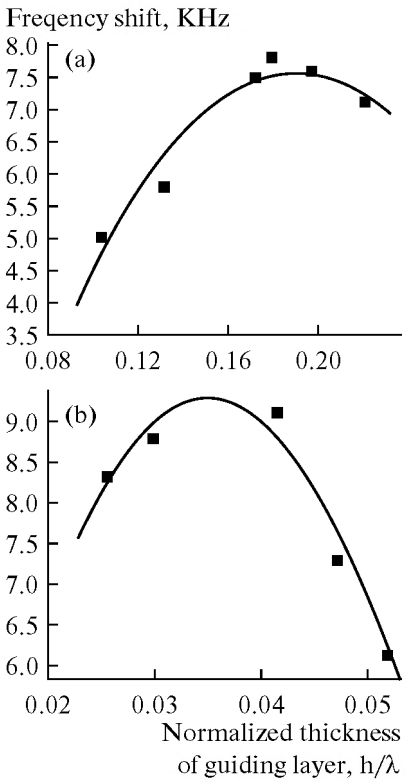

Fig. 3. Experimental frequency shift of Love-wave immunosensor versus normalized thickness of guiding layer: (a) SiO_2; (b) ZnO.

First, inject 100 μL 0.01 Mole phosphate buffer saline (PBS) of PH 7.4 into the cell to establish a frequency baseline. As the frequency of the Love wave immunosensor comes to stabilization, 10 μL PBS is moved away from the cell and then 10 μL of human IgG is injected into the cell by using a microsyringe. The performance of the immunosensor can be evaluated by recording frequency shift of the Love-wave device against time. Finally, the frequency responses of the Love-wave sensors with different guiding layer thicknesses to injection of 100 μg/mL H IgG are shown in Fig. 3. The experimental results of both Love-wave immunosensors show that the sensitivities (frequency shift) of the immunosensors are strongly dependent on the thicknesses of the guiding layers, although the thicknesses of the thin sensitive films also have a little influence. The sensitivities of the Love sensors increase firstly with thicknesses increase of the guiding layers, then decrease with the thicknesses further increase, and there are optimum thicknesses to get maximum sensitivities.

3. THEORY

A theoretical model of the Love-wave immunosensors with layered structures consists of a piezoelectric substrate, a guiding layer, a sensitive film and a liquid mass loading as shown in Fig. 4.

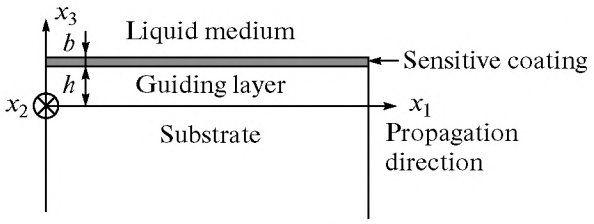

Fig. 4. Theoretical model of Love-wave immunosensors (x_1: propagation direction; x_2: polarization direction; x_3: depth direction).

In a piezoelectric medium, the applicable equations are the combinations of the elastic motion equations and Maxwell's equations, intercoupled by the piezo-electric tensors of the medium. Using the so-called "static-field approximation", the elastic wave equations for the particle displacements u_j along the coordinate axes x_j shown in Fig. 4 are intercoupled to the anisotropic Laplace's equation for the potential ϕ by the piezoelectric tensor e_{ijk}. So the particle displacements and the potential must satisfy the following equations [15]:

$$\begin{cases} \rho\dfrac{\partial^2 u_j}{\partial t^2} - c_{ijkl}\dfrac{\partial^2 u_k}{\partial x_i \partial x_i} - e_{kij}\dfrac{\partial^2 \phi}{\partial x_i \partial x_k} = 0 \\ e_{ikl}\dfrac{\partial^2 u_k}{\partial x_i \partial x_i} - \varepsilon_{ik}\dfrac{\partial^2 \phi}{\partial x_i \partial x_k} = 0 \quad (i,j,k,l = 1,2,3) \end{cases}, \quad (1)$$

where ρ is the density, c_{ijkl} are the elastic constants, and ε_{ik} are the dielectric permittivity tensors. Each tensor in Eq. (1) is referred to the coordinate system of Fig. 4 and the summation convention on repeated subscripts is applied.

The particle displacements and potential in Eq.(1) are assumed to be a linear combination of partial waves of the following form:

$$\begin{cases} u_j = \alpha_j \exp(ikbx_3)\exp[ik(x_1 - vt)] \\ \phi = \alpha_4 \exp(ikbx_3)\exp[ik(x_1 - vt)] \end{cases}, \quad (2)$$

α_j and α_4 stand for the relative amplitudes of the particle displacement and the potential respectively, k and v are the wave vector and phase velocity in x_1 direction respectively, and b gives the variation of the amplitude and phase of the partial wave in the depth (x_3) direction.

Substituting Eq.(2) into (1) gives the following "Christoffel equation":

$$\begin{bmatrix} \Gamma_{11} - \rho v^2 & \Gamma_{12} & \Gamma_{13} & \Gamma_{14} \\ \Gamma_{12} & \Gamma_{22} - \rho v^2 & \Gamma_{23} & \Gamma_{24} \\ \Gamma_{13} & \Gamma_{23} & \Gamma_{33} - \rho v^2 & \Gamma_{34} \\ \Gamma_{14} & \Gamma_{24} & \Gamma_{34} & \Gamma_{44} \end{bmatrix} \begin{bmatrix} \alpha_1 \\ \alpha_2 \\ \alpha_3 \\ \alpha_4 \end{bmatrix} = 0, \quad (3)$$

$$\Gamma_{11} = c_{11} + 2c_{15}b + c_{55}b^2, \quad \Gamma_{12} = c_{16} + (c_{14} + c_{56})b + c_{45}b^2,$$
$$\Gamma_{13} = c_{15} + (c_{13} + c_{55})b + c_{35}b^2,$$
$$\Gamma_{14} = e_{11} + (e_{15} + e_{31})b + e_{35}b^2,$$
$$\Gamma_{22} = c_{66} + 2c_{46}b + c_{44}b^2,$$
$$\Gamma_{23} = c_{56} + (c_{36} + c_{45})b + c_{34}b^2,$$
$$\Gamma_{24} = e_{16} + (e_{14} + e_{36})b + e_{34}b^2,$$
$$\Gamma_{33} = c_{55} + 2c_{35}b + c_{33}b^2,$$
$$\Gamma_{34} = e_{15} + (e_{13} + e_{35})b + e_{33}b^2,$$
$$\Gamma_{44} = -(\varepsilon_{33}b^2 + 2\varepsilon_{13}b + \varepsilon_{11}).$$

The physical parameters of 36°YX-$LiTaO_3$ piezoelectric substrates can be obtained through the related coordinate transform of the $LiTaO_3$ crystal.

In order to have nontrivial solutions, the determinant of the square matrix in Eq.(3) must equal to zero. Thus we achieve an eighth-order algebraic equation in the quantity b for a given phase velocity v, and hence there are eight roots. For each of the eight roots there is a four-component eigenvector (α_1, α_2, α_3, α_4).

Since the solutions represent Love waves, for the substrate, only the values of b lying within the lower half of the complex plane are retained, so as to ensure the solutions decay to zero with depth below the interface of the guiding layer and substrate. All eight values of b for the guiding layer and also eight for the sensitive film are retained because with a finite layer thickness, the solutions which decay, grow or remain constant with depth are all admissible. Thus there are four partial waves in the substrate and eight in the guiding layer and also eight in the sensitive film, all of which satisfy Eq. (1). These partial waves are in linear combinations with weighting factors chosen to satisfy the boundary conditions as follows:

In the substrate

$$\begin{cases} u_j = \left\{ \sum_{m-1}^{4} C_m \alpha_{jm} \exp(ikb^{(m)}x_3) \right\} \exp[ik(x_1 - vt)] \\ \phi = \left\{ \sum_{m-1}^{4} C_m \alpha_{4m} \exp(ikb^{(m)}x_3) \right\} \exp[ik(x_1 - vt)] \end{cases}, \quad (4)$$

while in the guiding layer

$$\begin{cases} \hat{u}_j = \left\{ \sum_{n-1}^{8} B_n \hat{\alpha}_{jn} \exp(ikb^{(n)}x_3) \right\} \exp[ik(x_1 - vt)] \\ \hat{\phi} = \left\{ \sum_{n-1}^{8} B_n \hat{\alpha}_{4n} \exp(ikb^{(n)}x_3) \right\} \exp[ik(x_1 - vt)] \end{cases}, \quad (5)$$

and in the sensitive film

$$\begin{cases} \tilde{u}_j = \left\{ \sum_{p-1}^{8} B_p \tilde{\alpha}_{jp} \exp(ikb^{(p)}x_3) \right\} \exp[ik(x_1 - vt)] \\ \tilde{\phi} = \left\{ \sum_{p-1}^{8} B_p \tilde{\alpha}_{4p} \exp(ikb^{(p)}x_3) \right\} \exp[ik(x_1 - vt)] \end{cases}. \quad (6)$$

The summation index "m" in Eq. (4) ranges over the four labels of the retained roots for the substrate, and the indexes "n" and "p" in Eq. (5) and Eq. (6) range over the eight labels of the eight roots for the guiding layer and sensitive film, respectively. "^" and "~" represent the material properties of the guiding layer and the sensitive film, respectively.

The boundary conditions involving three interfaces are as follows: on the interface between the substrate and guiding layer, the particle displacements, the stress, the potential and the normal component of the electrical displacement are in continuity; on the interface between the guiding layer and sensitive film, these four physical properties are also in continuity; then on the surface of the sensitive film, the continuity of the potential and the normal component of the electrical displacement is still kept, but considering the liquid medium as mass loading, the stress must satisfy:

$$\tilde{T}_{31} = -\rho_L h_L \ddot{\tilde{u}}_1, \quad \tilde{T}_{32} = -\rho_L h_L \ddot{\tilde{u}}_2, \quad \tilde{T}_{33} = -\rho_L h_L \ddot{\tilde{u}}_3, \quad (7)$$

where ρ_L and h_L are the density and thickness of the liquid layer.

Thus, based on the partial wave theory and boundary conditions, the phase velocity of the Love-wave devices and the sensitivity of the Love-wave immunosensor can be obtained using the numerical calculations if the mechanical, acoustical and geometrical parameters of the related materials are already determined.

4. THEORETICAL RESULT OF SENSITIVITY OF LOVE-WAVE IMMUNOSENSOR

At first, the elastic constants of the guiding layers are determined by fitting the calculation results of the phase velocities of the Love wave devices by above partial wave theory to the experimentally obtained data shown in Fig. 2. In the fitting the densities of the layers are assumed the same as that of the corresponding bulks, and then the best fitting elastic parameters are listed in Table 2.

Finally, using the theoretical model above, the sensitivities of the Love-wave immunosensors based on SiO_2/36°YX-$LiTaO_3$ and ZnO/36°YX-$LiTaO_3$ structures are calculated numerically. In the calculations, the physical parameters of 36°YX-$LiTaO_3$ piezoelectric substrates are obtained from the related coordinate transform for $LiTaO_3$ crystal based on "IEEE Standard on Piezoelectricity", the elastic parameters of the guiding layers are shown in Table 2 and then the sensitive film is assumed as

Table 2. Elastic constant of guiding layer

Material	SiO_2		ZnO				
Elastic constant, 10^{10} N/m^2	c_{11}	c_{44}	c_{11}	c_{33}	c_{44}	c_{12}	c_{13}
Bulk	7.85	3.12	20.97	21.09	4.25	12.11	10.51
Thin film	3.76	1.56	17.68	21.09	1.70	12.11	10.51

an isotropic material with the Lame's constants $\lambda = 1.68 \times 10^{10}$ N/m^2, $\mu = 0.08 \times 10^{10}$ N/m^2, and density $\rho = 1170$ kg/m^3, which are determined by the numerical simulations based on the parameters of PMMA [16].

The calculated results of the gravimetric sensitivities of the Love-wave immunosensors versus normalized guiding layer thicknesses are shown in Fig. 5. It can be seen that the calculated sensitivities variations with the normalized guiding layer thicknesses are essentially consistent with those of the experiments including the variation tendencies and the optimum thicknesses to get maximum sensitivities.

5. CONCLUSION

The Love-wave immunosensors based on SiO_2/36°YX-$LiTaO_3$ and ZnO/36°YX-$LiTaO_3$ structures are fabricated, and their sensing performances have been measured experimentally. Meanwhile, a theoretical model for the Love-wave immunosensors is built up using the partial wave theory of elastic waves propagating in three-layer structures covered by liquid loads. The sensitivities of the Love-wave immunosensors based on SiO_2/36°YX-$LiTaO_3$ and ZnO/36°YX-$LiTaO_3$ structures are calculated. The relationships between the sensitivities of the Love wave immunosensors and normalized thicknesses of the guiding layers are then obtained theoretically. Comparing the theoretical and experimental results, both are in agreements with each other.

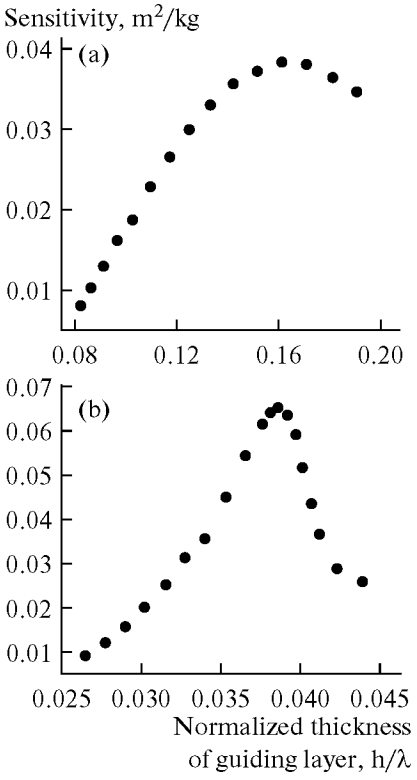

Fig. 5. Theoretical sensitivity of Love-wave sensor versus normalized thickness of guiding layer: (a) SiO_2; (b) ZnO.

ACKNOWLEDGMENTS

This work is supported by National Natural Science Foundation of China, No. 11174142, National Basic Research Program of China, No. 2012CB921504 and PAPD Project of Jiangsu Higher Education Institutions.

REFERENCES

1. M. J. Vellekoop, G. W. Lubking, P. M. Sarro, and A. Venema, Sens. Actuators A **43**, 175 (1994).
2. A. Rugemer, S. Reiss, A. Geyer, et al., Sens. Actuators B **56**, 45 (1999).
3. W. P. Jakubik, M. W. Urban'czyk, S. Kochowski, and J. Bodzenta, Sens. Actuators B **82**, 265 (2002).
4. M. D. Schlensog, T. A. Gronewold, M. Tewesa, et al., Sens. Actuators B **101**, 308 (2004).
5. E. Gizeli, N. J. Goddard, C. R. Lowe, and A. C. Stevenson, Sens. Actuators B 6, 131 (1992).
6. F. Herrmann, M. Weihnacht, and S. Büttgenbach, Ultrasonics **37**, 335 (1999).
7. C. Zimmermann, D. Rebiere, C. Dejous, et al., Sens. Actuators B **86**, 76 (2001).
8. A. C. Turton, D. Bhattacharyya, and D. Wood, Sens. Actuators A **123–124**, 267 (2005).
9. J. Du, G. L. Harding, and J. A. Ogilvy, Sens. Actuators A **56**, 211 (1996).
10. K. K. Zedeh, A. Trinchi, W. Wlodarski, and A. Holland, Sens. Actuators A **100**, 135 (2002).
11. R. C. Chang, S. Y. Chu, C. S. Hong, and Y. T. Chuang, Thin Solid Films **498**, 146 (2006).
12. F. M. Zhou, Z. Li, L. Fan, and S. Y. Zhang, Ultrasonics **50**, 411 (2010).
13. Y. Wang, S. Y. Zhang, F. M. Zhou, et al., Sens. Actuators B **158** 97 (2011).
14. S. W. Wenzei and R. M. White, Appl. Phys. Lett. **54**, 1976 (1989).
15. G. W. Farnell and E. L. Adler, in *Physical Acoustics, Vol. 9*, Ed. by W. P. Mason and R. N. Thurston, (Academic, New York, 1972), pp. 35–126.
16. O. Tamarin, C. Dejous, and D. Rebiere, Sens. Actuators B **91**, 275 (2003).